Unusual feature of α spectra in the $^{12}C + ^{93}Nb$ reaction near Coulomb barrier energies

E. T. Mirgule,[1] D. R. Chakrabarty,[1] V. M. Datar,[1] Suresh Kumar,[1] A. Mitra,[1] V. Nanal,[2] and P. C. Rout[1]

[1]*Nuclear Physics Division, Bhabha Atomic Research Centre, Mumbai 400085, India*

[2]*Tata Institute of Fundamental Research, Mumbai 400005, India*

(Received 6 April 2010; revised manuscript received 19 October 2010; published 23 December 2010)

Proton and α-particle spectra have been measured at backward angles in the $^{12}C + ^{93}Nb$ reaction at $E(^{12}C) =$ 37.5–60 MeV and in the $^{16}O + ^{93}Nb$ reaction at $E(^{16}O) =$ 54–75 MeV. The inclusive particle spectra generally are in good agreement with the statistical model calculations except for the α spectra in the ^{12}C-induced reaction at beam energies of 37.5–42.5 MeV which are close to the Coulomb barrier in the entrance channel. In these cases the evaporation peak is up to 2 MeV lower than its expected position from the statistical model predictions. Gamma-multiplicity-gated α spectra, measured in the same reaction, also show the aforementioned discrepancy. These observations reveal that the conventional statistical model cannot explain the α-particle spectra in the ^{12}C-induced reactions near the Coulomb barrier.

DOI: 10.1103/PhysRevC.82.064608 PACS number(s): 25.70.Gh, 24.10.Pa

I. INTRODUCTION

The study of the decay properties of hot rotating nuclei produced in heavy-ion fusion reactions is an active field of research. The compound nuclei (CN) formed at different excitation energies and angular momenta decay by the evaporation of light particles and γ rays. The statistical model (SM) [1–3] has been used to understand the evaporation energy spectra. The shapes of the spectra are determined mainly by the excitation energy and angular momentum dependence of the nuclear level density in the residual nuclei and the transmission coefficients of the emitted particles. The effective barrier, consisting of the Coulomb and the centrifugal part, decides the shape of the lower energy part of the evaporation spectrum including the evaporation peak. The sizes and shapes of the emitting nuclei influence the effective emission barriers, and a measurement of these spectra, therefore, can provide valuable information about these parameters.

A number of measurements on the particle spectra over a range of projectile-target combinations have been reported in the literature. Although the measured spectra generally agree with SM calculations, there are significant discrepancies particularly for the α-particle spectra. Several experimental studies at high excitation energies and angular momenta have found that the measured spectra are enhanced in the sub-barrier region (the barrier referring to the Coulomb barrier in the α-residual nucleus system) and the evaporation peak energies are lower than the SM [3–5] predictions. The SM calculations use transmission coefficients obtained from the inverse process of absorption of an α particle by a nucleus in the ground state. The sub-barrier enhancement indicates a reduction in the emission barrier which, in turn, implies deformation of the composite system at high angular momenta and excitation energies. The deformation also modifies the nuclear level density [4–6] needed in the SM calculation. Calculations have also been performed considering a distribution of nuclear shapes [7] arising due to the thermal fluctuation. An alternative explanation of the sub-barrier enhancement has been suggested as due to the emission of unstable clusters that subsequently decay producing sub-barrier α particles [8].

Most of the discrepancies mentioned previously are reported at beam energies well above the Coulomb barrier (CB) of the projectile-target system. At these energies, contributions from other reaction mechanisms, such as incomplete fusion, breakup, etc., also become increasingly important [9]. At energies around the CB, the complete fusion mechanism is expected to be dominant. In addition, since the angular momentum brought in is low at these energies, the complications arising from the spin-induced deformation should also be less important. However, not much data is available at very low beam energies.

We have recently reported [10] measurements of α spectra in $^{12}C + ^{93}Nb$ and $^{12}C + ^{58}Ni$ reactions at ^{12}C beam energies of 40 and 50 MeV and in the $^{16}O + ^{93}Nb$ reaction at ^{16}O beam energy of 75 MeV. It was observed that in the case of the $^{12}C + ^{93}Nb$ reaction at 40 MeV, which is near the CB in the entrance channel, the evaporation peak is $\sim$2 MeV lower in energy compared to the calculation based on the SM. The agreement was good at 50 MeV beam energy. No such discrepancy was observed in the case of other reactions. This discrepancy could imply that the α-particle emission takes place from a deformed configuration at near-barrier energies. On the other hand, it could be due to an unexpectedly large contribution from the noncompound processes mentioned earlier. The motivation of the present work is to get more insight into this discrepancy from a measurement of the beam energy dependence of the particle spectra. In this work, the proton and α spectra were measured for two systems $^{12}C + ^{93}Nb$ and $^{16}O + ^{93}Nb$ at near and above Coulomb barrier energies. The spectra were also measured in coincidence with a low-energy γ multiplicity array to assess the effect of angular momentum on the measured spectra.

II. EXPERIMENTAL DETAILS

The experiment was performed at the 14UD BARC-TIFR Pelletron Laboratory in Mumbai. The proton and α-particle spectra were measured in the $^{12}C + ^{93}Nb$ reaction at ^{12}C beam energies of 37.5, 40, 42.5, 45, 50, and 60 MeV and in the

$^{16}O + ^{93}Nb$ reaction at ^{16}O beam energies of 54, 60, and 75 MeV. The target was a self-supporting ^{93}Nb foil of thickness $\sim$0.5 mg/cm^2. Protons and α particles were detected using three silicon surface barrier ΔE-E telescopes with thickness combinations of (30 μm + 1 mm), (30 μm + 2 mm), and (25 μm + 2 mm). These telescopes were kept at backward angles of 116°, 125°, and 153° and at a distance of 6.6 cm from the target. The solid angle subtended by each telescope was $\sim$22 mSr. The measurements were done at backward angles to minimize the spectral contamination from light impurities mainly due to carbon buildup and the oxygen content in the target. Nevertheless, the contributions from these impurities were subtracted. For this purpose, proton and α spectra were measured using a carbon ($\sim$30 μg/cm^2) and a WO_3 ($\sim$80 μg/cm^2) target at each of the corresponding beam energies. These spectra were normalized and subtracted from the main spectra. The normalization factors were deduced from the yields of monoenergetic characteristic α groups from ^{12}C and ^{16}O nuclei. A Si telescope (50 μm + 2 mm) was placed at an angle of 10° and at a distance of 5.5 cm from the target for the measurement of these α groups from all the three targets. More details are described in Ref. [11].

Measurements of the particle spectra were also made in coincidence with the low-energy γ rays emitted from the residual nuclei populated below the particle emission threshold. The multiplicty of these γ rays are related to the angular momentum populated in the compound system. These were detected in a 14-element bismuth germanate (BGO) multiplicity array [12]. The efficiency of this array was measured to be $\sim$62% for 662 keV γ rays using a calibrated ^{137}Cs source placed at the target position. The number of BGO detectors in coincidence with the charged particle detectors, henceforth called fold (F), was recorded in an event-by-event mode in a Computer Automated Measurement and Control (CAMAC)-based multiparameter data acquisition system. The trigger for data recording was generated from the timing signal from any one of the three telescopes. The telescopes were calibrated using elastically scattered protons from a 1 mg/cm^2 thick ^{209}Bi target at proton beam energies of 17, 19, and 22 MeV. The radioactive $^{241}Am + ^{239}Pu$ and ^{229}Th α sources were used for low energies from 5 to 8 MeV. The stability of energy calibration was monitored by using a precision pulser during the measurements.

III. DATA ANALYSIS AND EXPERIMENTAL RESULTS

Two-dimensional spectra of BGO fold versus energy (deposited in the E detector) were generated for protons and α particles at each beam energy after putting appropriate software gates on the raw data for particle identification. The inclusive spectra were created from a full projection of the two-dimensional spectra on the energy axis whereas the fold-gated spectra were obtained from a projection for the corresponding folds. The laboratory energy spectra were derived from the projected spectra after taking into account the energy loss in the ΔE detectors. This was calculated using the stopping power parameterization of Ref. [13]. The laboratory spectra were converted into the center of mass (c.m.) spectra. The angle-integrated spectra were derived after multiplying

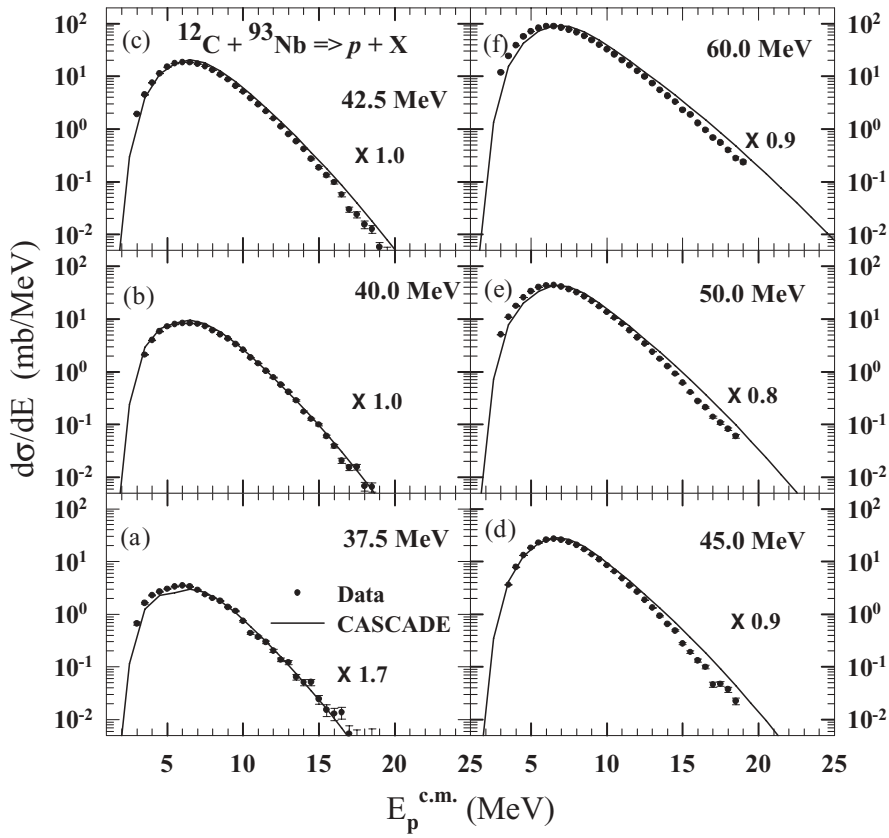

FIG. 1. Inclusive proton spectra in the $^{12}C + ^{93}Nb$ reaction at various beam energies shown in the figure. $E_p^{c.m.}$ is the proton energy in the c.m. system. The solid lines show the results of CASCADE calculations after multiplication by the factors (see text) indicated in the figure.

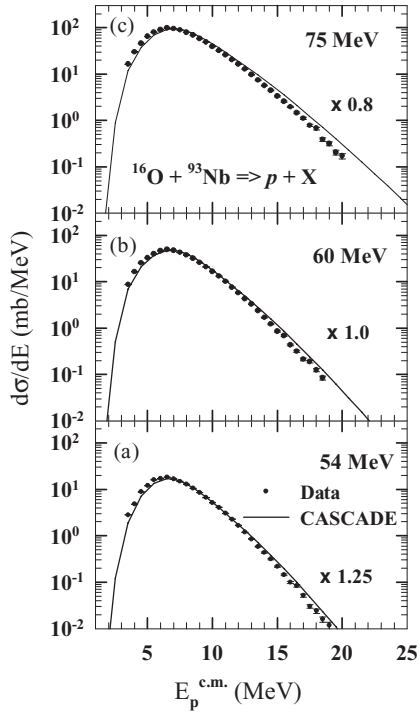

FIG. 2. As in Fig. 1, for the ^{16}O + ^{93}Nb reaction.

by the appropiate weightage factors and summing the data at different angles. The derived spectra agree in shape with those reported earlier [10,15] (for the cases that are common to the present study) but differ in absolute value by a factor of ∼1.6. Whereas the exact reason for this systematic error could not be ascertained, we have multiplied all spectra by a factor of 1.6 for the further analysis discussed below.

A. Inclusive spectra and statistical model analysis

The final inclusive c.m. spectra for protons and α's are shown in Figs. 1–4. These spectra were compared with the results of the statistical model calculation using the computer code CASCADE [14]. The important ingredients in the calculations are the angular momentum distribution in the compound nucleus along with the fusion cross section, the level densities of the residual nuclei, and the transmission coefficients of emitted particles. The fusion cross sections were calculated using the coupled-channel computer program CCFUS [16] including the coupling between the elastic and inelastic channels for both target and projectile excitations. The program also gives the orbital angular momentum ($l\hbar$) distribution in the compound nucleus. These distributions could be described as

$$P(l) \sim \frac{(2l+1)}{1+\exp[(l-l_0)/\delta_l]},$$

where l_0 denotes the critical angular momentum for fusion and δ_l is the diffuseness parameter. The fusion cross sections and the parameters l_0 and δ_l are shown in Table I. For the calculation of the excitation energy and the angular momentum dependence of the nuclear level densities, the prescription of Ignatyuk *et al.* [17] was used with the asymptotic level density parameter $\tilde{a} = A/8.5$, where A is the mass number

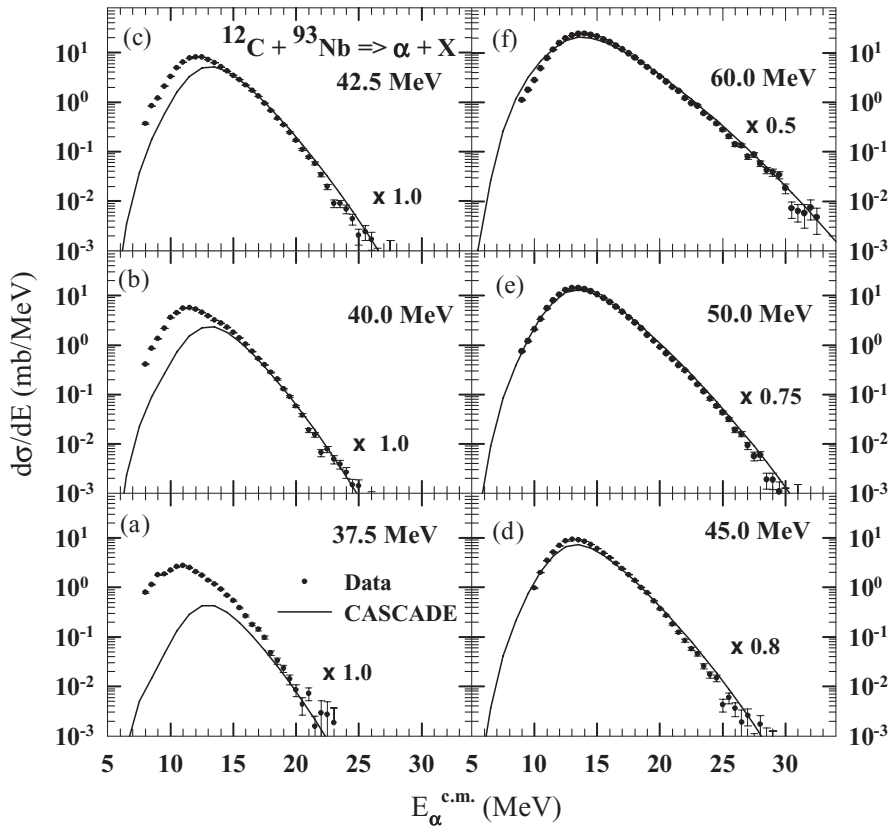

FIG. 3. Inclusive α spectra in the ^{12}C + ^{93}Nb reaction at various beam energies shown in the figure. $E_\alpha^{c.m.}$ is the α energy in the c.m. system. The solid lines show the results of CASCADE calculations after multiplication by the factors (see text) indicated in the figure.

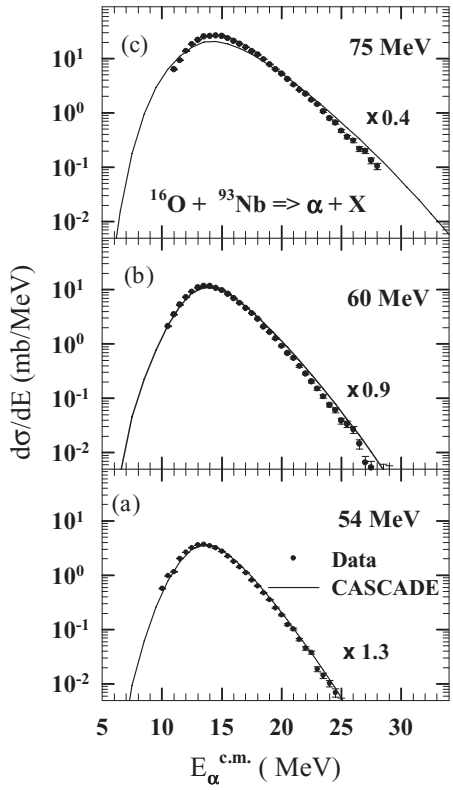

FIG. 4. As in Fig. 3, for the $^{16}O + ^{93}Nb$ reaction.

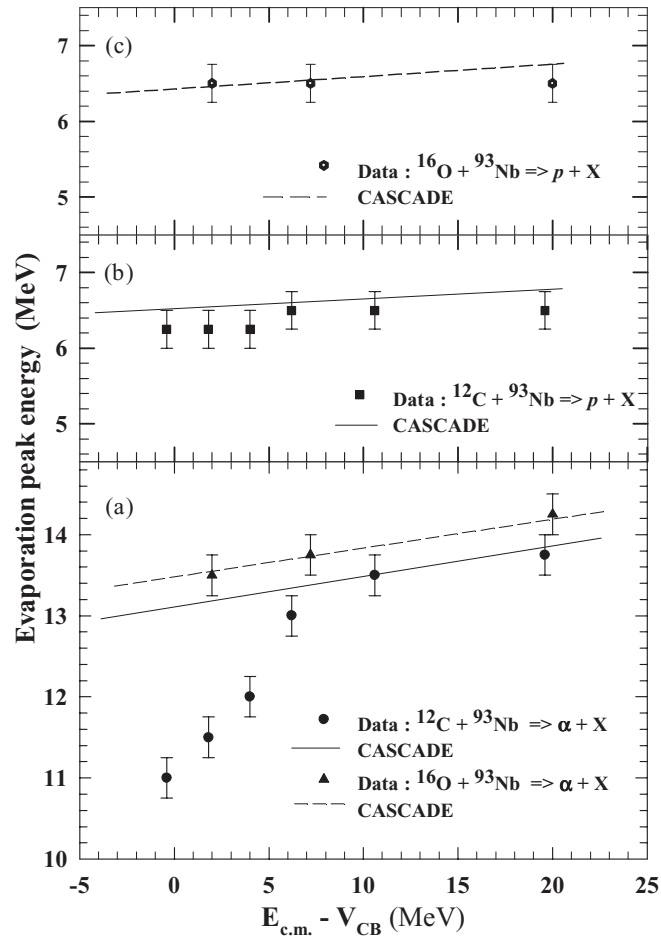

FIG. 5. Variation of observed evaporation peak energy in α (a) and proton (b, c) spectra with beam energy (in c.m.) above the Coulomb barrier in the entrance channel. The solid and dashed lines are the CASCADE predictions.

of the nucleus. The transmission coefficients were calculated using the corresponding optical model potentials. The optical potential parameters for n, p, and α were taken from Refs. [18–21]. The calculated statistical model spectra are shown in Figs. 1−4 by solid lines after multiplying by the factors indicated in the figures. These somewhat arbitrary factors were chosen so as to generally reproduce the overall cross sections.

In the case of protons (Figs. 1 and 2), the comparison of the calculated spectra with the measured ones shows that the shapes of the spectra agree reasonably well with the experimental data for all the cases. The same is true for the α spectra for the $^{16}O + ^{93}Nb$ system (Fig. 4). However, the α spectra for the $^{12}C + ^{93}Nb$ system at beam energies of 37.5, 40, and 42.5 MeV [Figs. 3(a)–3(c)] show a significant discrepancy in the position of the evaporation peaks. The SM calculation gives the peak energy at ∼2 MeV above the experimental value for the lowest beam energy of 37.5 MeV. The discrepancy gradually decreases with the increase in beam energy and the data agree reasonably with the calculations beyond the beam energy of 45 MeV. This interesting result is graphically presented in Fig. 5. The observed evaporation

TABLE I. Relevant parameters for the systems studied. E_{lab} is the beam energy at the target center, $E_{c.m.}$ is the corresponding c.m. energy, V_{CB} is the Coulomb barrier in c.m. and σ_{fus} is the fusion cross section. Other parameters are described in the text.

System	V_{CB} (MeV)	E_{lab} (MeV)	σ_{fus} (mb)	$E_{c.m.}$-V_{CB} (MeV)	l_o	δ_l
		37.1	38.3	−0.4	5.6	1.8
		39.6	178	1.8	10.2	1.5
$^{12}C + ^{93}Nb$	33.3	42.1	343	4.0	14.5	1.3
		44.6	498	6.2	17.8	1.1
		49.6	769	10.6	23.4	0.9
		59.7	1175	19.6	31.5	0.8
		53.3	137	2.0	13.5	1.6
$^{16}O + ^{93}Nb$	43.5	59.4	465	7.2	22.8	1.3
		74.4	1041	20.0	37.0	1.0

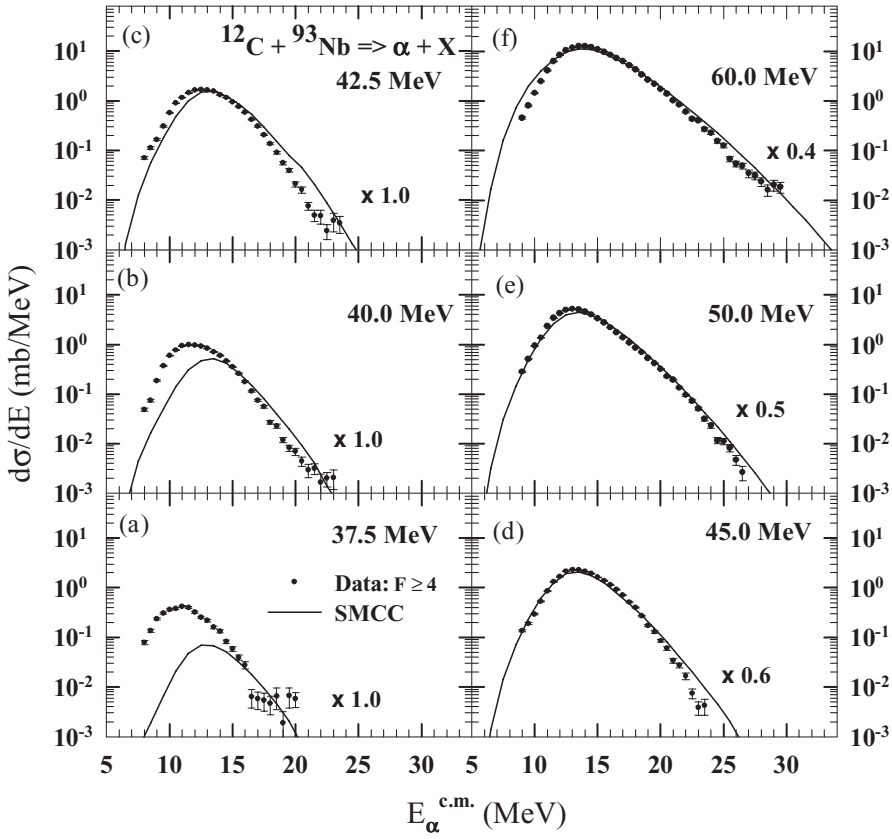

FIG. 6. Fold-gated α spectra in the $^{12}C + ^{93}Nb$ reaction at various beam energies along with the results of SMCC calculations (see text) for fold $F \geqslant 4$ after multiplication by the factors indicated in the figure. $E_\alpha^{c.m.}$ is the α energy in the c.m. system.

peak energies are plotted against the beam energy (in the c.m. system) above the Coulomb barrier V_{CB} [22] for the α [Fig. 5(a)] and proton [Figs. 5(b)–5(c)] spectra. The V_{CB} values obtained from the output of the CCFUS program are shown in Table I. The CASCADE predictions of the evaporation peak energies are shown in Fig. 5 as solid and dashed lines.

It is worthwhile at this point to address the variation of the evaporation peak energy with the input parameters in the CASCADE calculations. The calculations were performed for different level density parameters, optical potentials, and the input angular momentum distribution in the entrance channel. A change in the level density parameter from $A/7.5$ to $A/9.5$ was seen to change the evaporation peak energy by $\sim$0.2 MeV. A variation of l_0 by an arbitrary factor of $\sim$1.4 changed the peak energy by $\sim$0.1 MeV whereas the δ_l values between 0 to 4 yielded a change of $\sim$0.3 MeV. Different choices of the optical potential parameters as given in the CASCADE code were also tried. The change in evaporation peak energy was again less than 0.2 MeV. Thus, under the assumption that the α-particle spectra originate from the compound nuclear evaporation process, the present results demonstrate unusual features in the ^{12}C-induced reactions. A reduction in the effective emission barrier for the α particle, incorporated via an artificial increase in the radius parameter in the optical potential, can explain the data as was shown in our earlier work [10]. This could be indicative of an unusual large deformation of the excited CN at low angular momenta.

B. Fold gated spectra and statistical model analysis

One component of the present work was to investigate the effect of angular momentum on the evaporation peak discrepancy. It may be emphasized that any possible effect due to light impurities should decrease with increase in the fold (defined earlier) which is related to the angular momentum in the compound system. The fold-gated α spectra are shown in Figs. 6 and 7 for $F \geqslant 4$. These spectra were also compared with the statistical model calculations. The fold-gated spectra cannot be calculated with the CASCADE code in a straightforward manner. A simulated Monte Carlo CASCADE (SMCC) code [23] was used for this purpose. The SMCC code calculates the residue spin ($\hbar J_{res}$) distributions in different nuclei as a function of the evaporated particle energies. A J_{res} to F response function is calculated for all the residues by considering the γ-decay cascade to the ground state. The multiplicity of the γ rays in each decay chain is then converted to F distribution after incorporating the efficiency of the multiplicity detectors and the cross talk probabilities in a Monte Carlo approach. By convoluting the J_{res} distribution with these response functions, a $\sigma(E_p, F)$ matrix (the cross section distribution as function of particle energy E_p and F) is calculated. Suitable projections of this matrix on the E_p axis give F-gated particle spectra. It may be worth mentioning that for a fold condition of $F \geqslant 4$, the average J_{res} values range from $\sim$10 to 18 for the $^{12}C + ^{93}Nb$ reaction and from $\sim$12 to 20 for the $^{16}O + ^{93}Nb$ reaction, for the present range of beam energies. The full width at

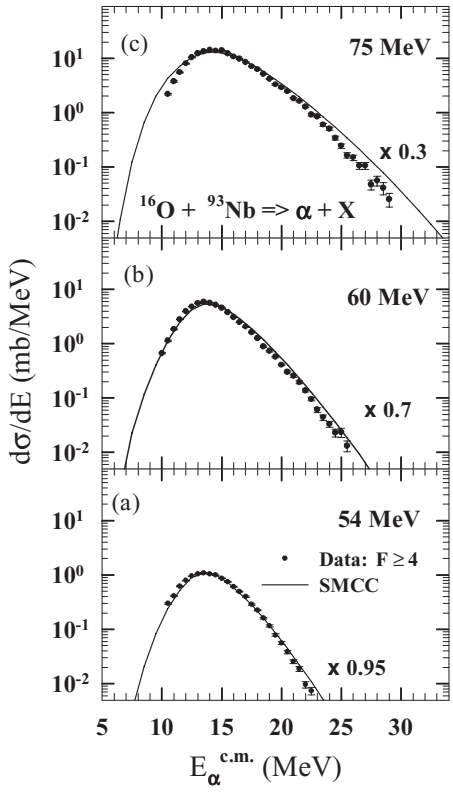

FIG. 7. As in Fig. 6, for the $^{16}O + ^{93}Nb$ reaction.

half maximum values vary between 6 to 11 and 7 to 11, respectively.

The solid lines in Figs. 6 and 7 show the results of the SMCC calculations for the fold-gated ($F \geqslant 4$) α spectra in the $^{12}C + ^{93}Nb$ and $^{16}O + ^{93}Nb$ reactions, respectively, at all the beam energies. A comparison with the experimental spectra show that the SMCC calculations reasonably reproduce the overall shapes of the spectra in the $^{12}C + ^{93}Nb$ reaction at beam energies of 45 to 60 MeV and in the $^{16}O + ^{93}Nb$ reaction at all beam energies. However, the calculations are unable to reproduce the observed features for the $^{12}C + ^{93}Nb$ reaction at lower energies as in the case of the inclusive spectra. This implies that the evaporation peak discrepancy is not affected by angular momentum in the compound nucleus.

IV. DISCUSSION

The comparison of the present experimental data with the statistical model calculations shows a significant discrepancy in the case of α spectra in the $^{12}C + ^{93}Nb$ reaction at beam energies close to the Coulomb barrier. On the generally accepted assumption that at low energies complete fusion should be the most important process, the observed discrepancy could imply α-particle emission from a deformed configuration as mentioned earlier. In the experiments at higher beam energies, the observed lowering of the effective α emission barrier has been conjectured [4,5,7] to be due to the angular-momentum-driven deformed configurations formed during the fusion process. The nuclei populated in the present studies are near spherical as can be deduced from their low-lying energy spectra. The angular momenta and the excitation energies populated in the compound system, particularly for near-barrier beam energies, are also low and should not lead to a significant shape transition or shape fluctuation [7]. Therefore, these shape-related effects on the α-particle spectra, generally important at higher beam energies, should not be responsible for the observed discrepancy in the present case. However, the dynamics of the entrance channel can lead to a distribution of Coulomb barriers [24,25] that is known to play an important role in the near-barrier fusion processes. The processes can be very different depending on the structure of the projectile and/or the target. It is possible that the compound system is formed by the fusion through a very deformed configuration and subsequently takes time for full equilibration in all degrees of freedom. If this shape survives sufficiently long for α particles to be emitted, it can lead to the enhanced α-particle emission of lower energies, making the evaporation peak shift to a lower energy value. Such a scenario might be helped by the fact that ground-state wave function of ^{12}C has a significant component of the highly deformed cluster state [26] at 7.65 MeV, which could be excited in the intermediate stages before the complete fusion. The observed agreement in the case of proton spectra, however, can be reconciled to only if we assume that the proton emission takes place mostly after the full equilibration. Also, the observed agreement for α spectra at above-barrier beam energies then would imply that the formation and survival of the deformed shapes is less probable at higher beam energies. In the case of the $^{16}O + ^{93}Nb$ reaction no such discrepancy is observed even at near barrier energies, possibly because there is no highly deformed cluster state admixture in the ground state of ^{16}O.

A very different explanation for the observed discrepancy could be due to a significant contribution from the processes other than the complete fusion. It may be noted that in the $^{12}C + ^{93}Nb$ reaction, the incomplete fusion (ICF) has been observed down to the beam energy of $E(^{12}C) \sim 47$ MeV [27,28]. The discrepancy between the observed cross sections of the present work and the statistical model predictions could be ascribed to the ICF process or the transfer of the ^{8}Be cluster to the continuum states in the final nucleus. The estimated cross sections for such processes, taken as the difference between the measured and the SM predictions, are not inconsistent with a low-energy extrapolation of the ICF cross sections reported in Refs. [27,28]. The agreement of the measured spectra with SM predictions at higher beam energies would mean that the processes become forward peaked and do not contribute to the back-angle data. However, for the $^{16}O + ^{93}Nb$ reaction, the present data do not require any contributions from a noncompound process even at the beam energy close to the Coulomb barrier. Thus the observed feature appears to be specific only to the ^{12}C-induced reaction at near-barrier energies. Again the intermediate excitation of the highly deformed cluster state in ^{12}C could contribute to the phenomenon.

Another possible explanation of the observed discrepancy can be the breakup of ^{12}C nuclei in the vicinity of the target after excitation to the 7.65-MeV state. This excitation energy is just above the 3α breakup threshold of 7.275 MeV.

The breakup α particles reaching the detector can create an apparently shifted evaporation peak energy in the spectrum. However, this process is not expected to produce high spin states in the residual system and should lead to a reduced γ multiplicity compared to the other processes. Therefore, the observation of the evaporation peak discrepancy even for high γ multiplicity ($F \geqslant 4$) is not very consistent with this explanation.

It may be mentioned that a different kind of unusual feature was recently observed by us in the fold-gated α spectra [15] in the $^{12}C + ^{93}Nb$ reaction. In that study, an unusual broad structure appeared at the higher energy part in the fold-gated spectra at the same beam energies as in this work. These structures also could not be understood by statistical model calculations. It is possible that there is some partial commonality between these two observations in terms of the noncompound cluster transfer processes. More systematic and exclusive measurements are needed to understand the special role, if any, played by the ^{12}C projectile in low-energy heavy-ion reactions.

V. SUMMARY

In summary, proton and α-particle spectra, both inclusive and fold gated, have been measured at backward angles in the reactions $^{12}C + ^{93}Nb$ at $E(^{12}C) = 37.5$–60 MeV and in $^{16}O + ^{93}Nb$ at $E(^{16}O) = 54$–75 MeV. The spectra were compared with the statistical model calculations on the well-accepted assumption that the compound nuclear process should be the most important process at low beam energies. The calculated inclusive spectra are generally in agreement with experimental data. However, there is a significant discrepancy for the α spectra in the $^{12}C + ^{93}Nb$ reaction at 37.5, 40, and 42.5 MeV. The experimental evaporation peak energy is $\sim$2 MeV lower for the beam energy of 37.5 MeV and gradually increases with beam energy, agreeing reasonably well beyond the beam energy of 45 MeV. The discrepancy is beyond the possible uncertainties of the statistical model prediction due to the variation in the input parameters. Similar discrepancies are also seen in the fold-gated α spectra implying, first, that any low-Z impurity in the target is not responsible for the observation and, second, that the observation is not dependent on the angular momentum. Since the angular momenta and the excitation energies populated in the compound system, particularly for near-barrier beam energies, are low, the effect of the shape transition or shape fluctuation of the compound system should not be responsible for the observed discrepancy. If the complete fusion is the dominant process at these low energies, the present observations would imply the emission of α particles from a very deformed complex before full equilibration. This should be, however, specific only to the ^{12}C projectile and the α spectra. The role played by the excited α-cluster configuration in ^{12}C prior to complete equilibration could be responsible for these observations. It is also possible to ascribe the observed discrepancies to noncompund nuclear processes like the incomplete fusion or the transfer to continuum. However, the ^{16}O-induced reactions do not need a contribution from this process even at the near-barrier beam energy indicating an unusual feature for the ^{12}C projectile. The breakup of ^{12}C into three α particles creating a displaced evaporation peak is in principle possible although it seems less probable because of the persistence of the discrepancy even for higher γ-ray multiplicity.

ACKNOWLEDGMENTS

The authors thank the Mumbai Pelletron accelerator staff for the smooth operation of the machine during the experiment.

[1] V. F. Weisskopf and D. H. Ewing, Phys. Rev. **57**, 472 (1940).
[2] W. Hauser and H. Feshbach, Phys. Rev. **87**, 366 (1952).
[3] R. G. Stokstad, in *Treatise on Heavy Ion Science*, edited by D. A. Bromley (Plenum, New York, 1985), Vol. 3, p. 83.
[4] G. Viesti, B. Fornal, D. Fabris, K. Hagel, J. B. Natowitz, G. Nebbia, G. Prete, and F. Trotti, Phys. Rev. C **38**, 2640 (1988).
[5] R. J. Charity *et. al.*, Phys. Rev. C **63**, 024611 (2001).
[6] J. R. Huizenga, A. N. Behkami, I. M. Govil, W. U. Schroder, and J. Toke, Phys. Rev. C **40**, 668 (1989).
[7] R. J. Charity, Phys. Rev. C **61**, 054614 (2000).
[8] R. J. Charity, M. Korolija, D. G. Sarantites, and L. G. Sobotka, Phys. Rev. C **56**, 873 (1997).
[9] Devendra P. Singh *et al.*, Phys. Rev. C **81**, 054607 (2010), and references therein.
[10] E. T. Mirgule, D. R. Chakrabarty, V. M. Datar, Suresh Kumar, A. Mitra, and H. H. Oza, Pramana J. Phys. **67**, 369 (2006).
[11] D. R. Chakrabarty, V. M. Datar, Suresh Kumar, E. T. Mirgule, H. H. Oza, and U. K. Pal, Phys. Rev. C **51**, 2942 (1995).
[12] A. Mitra, D. R. Chakrabarty, V. M. Datar, Suresh Kumar, E. T. Mirgule, and H. H. Oza, Nucl. Phys. A **707**, 343 (2002).
[13] H. H. Anderson and J. F. Ziegler, *The Stopping Power and Ranges of Ions in Matter* (Pergamon, New York, 1977), vol. 1.
[14] F. Puhlhofer, Nucl. Phys. A **280**, 267 (1980).
[15] A. Mitra, D. R. Chakrabarty, V. M. Datar, Suresh Kumar, E. T. Mirgule, V. Nanal, and P. C. Rout, J. Phys. G **36**, 095103 (2009).
[16] C. H. Dasso and S. Landowne, Comput. Phys. Commun. **46**, 187 (1987).
[17] A. V. Ignatyuk, G. N. Smirenkin, and A. S. Tishin, Sov. J. Nucl. Phys. **21**, 255 (1975).
[18] D. Wilmore and P. E. Hodgson, Nucl. Phys. **55**, 673 (1964).
[19] F. G. Perey, Phys. Rev. **131**, 745 (1963).
[20] J. R. Huizenga and G. Igo, Nucl. Phys. **84**, 177 (1966).
[21] L. Mcfadden and G. R. Satchler, Nucl. Phys. **84**, 177 (1966).
[22] R. A. Broglia and A. Winther, *Heavy Ion Reactions* (Addison-Wesley, Redwood City, 1991), Vol. 1, p. 116.
[23] D. R. Chakrabarty, Nucl. Instrum. Methods Phys. Res. A **560**, 546 (2006).

[24] N. Rowley, Pramana J. Phys. **53**, 495 (1999).
[25] M. Dasgupta, D. J. Hinde, N. Rowley, and M. Stefanani, Annu. Rev. Nucl. Part. Sci. **48**, 401 (1998).
[26] A. Arima, H. Horiuchi, K. Kubodera, and N. Takigawa, *Advances in Nuclear Physics* (Plenum, New York, 1972), Vol. 5, p. 345.
[27] B. S. Tomar, A. Goswami, A. V. R. Reddy, S. K. Das, P. P. Burte, S. B. Manohar, and Satya Prakash, Z. Phys. A **343**, 223 (1992).
[28] B. S. Tomar, A. Goswami, A. V. R. Reddy, S. K. Das, P. P. Burte, S. B. Manohar, and Bency John, Phys. Rev. C **49**, 941 (1994).